Current Biology, Vol. 15, 765–770, April 26, 2005, ©2005 Elsevier Ltd All rights reserved. DOI 10.1016/j.cub.2005.02.065

IP_3 Receptor Activity Is Differentially Regulated in Endoplasmic Reticulum Subdomains during Oocyte Maturation

Michael J. Boulware and Jonathan S. Marchant*
Department of Pharmacology
University of Minnesota
Minneapolis, Minnesota, 55455

Summary

Fertilization competency results from hormone-induced remodeling of oocytes into eggs. The signaling pathways that effect this change exemplify bistability, where brief hormone exposure irrevocably switches cell fate. In *Xenopus*, changes in Ca^{2+} signaling epitomize such remodeling: The reversible Ca^{2+} signaling phenotype of oocytes rapidly adapts to support irreversible propagation of the fertilization Ca^{2+} wave. Here, we simultaneously resolved IP_3 receptor (IP_3R) activity with endoplasmic reticulum (ER) structure to optically dissect the functional architecture of the Ca^{2+} release apparatus underpinning this reorganization. We show that changes in Ca^{2+} signaling correlate with IP_3R redistribution from specialized ER substructures called annulate lamellae (AL), where Ca^{2+} release activity is attenuated, into IP_3R-replete patches in the cortical ER of eggs that support the fertilization Ca^{2+} wave. These data show: first, that IP_3R sensitivity is regulated with high spatial acuity even between contiguous ER regions; and second, that drastic reorganization of Ca^{2+} signaling dynamics can be driven by subcellular redistribution in the absence of changes in channel number or molecular or familial Ca^{2+} channel diversity. Finally, these results define a novel role for AL in Ca^{2+} signaling. Because AL are prevalent in other scenarios of rapid cell division, further studies of their impact on Ca^{2+} signaling are warranted.

Results and Discussion

An appreciation of the functional versatility of cytoplasmic Ca^{2+} signaling necessitates a mechanistic understanding both of upstream events that generate different spatiotemporal patterns of Ca^{2+} release (i.e., how the "functional architecture" of Ca^{2+} signaling is established) and of the downstream functional consequences (i.e., how Ca^{2+} signals are decoded to regulate specific events). For dissection of the former, emphasis has correctly been placed on understanding flexibility provided via molecular diversity (expression of different Ca^{2+} channel isoforms with discrete behaviors) as well as familial diversity (expression of different Ca^{2+} channel families to provide multiple pathways for Ca^{2+} release/entry). However, the *Xenopus* oocyte expresses only a single isoform of a single family of the intracellular Ca^{2+} channel—a type-1-like IP_3 receptor (IP_3R, [1, 2]). Furthermore, during progesterone-induced maturation, there is little change in IP_3R abundance (~1.2-fold, [3]), despite changes in macroscopic Ca^{2+} signaling dynamics and ER structure previously visualized in separate functional or structural studies [4–6].

To dissect how this functional remodeling occurs, we used dual-emission, video-rate confocal imaging to simultaneously correlate ER structure with localized IP_3R properties in live cells. First, we injected cDNA into oocyte nuclei to express a red-fluorescent protein targeted to the ER lumen (DsRed2-ER). DsRed2-ER-expressing cells were subsequently injected with dextran-linked fluorescent Ca^{2+} indicators with affinities appropriate for comparing local or global Ca^{2+} signals. For example, to resolve the localization and properties of Ca^{2+} release sites, we used high-affinity Ca^{2+} indicators to characterize "Ca^{2+} puffs"—local Ca^{2+} signals that represent the activity of IP_3R clusters dispersed throughout the ER in oocytes [7]. DsRed2-ER-expressing cells injected with a Ca^{2+} indicator were then incubated with or without progesterone (eggs versus oocytes) to correlate ER morphology with Ca^{2+} dynamics.

Changes in Ca^{2+} Signaling Dynamics between *Xenopus* Oocytes and Eggs

First, we defined the spatiotemporal properties of Ca^{2+} signals in oocytes and eggs within the vegetal hemisphere, where major ER remodeling occurs during maturation [5]. When we used a high-affinity Ca^{2+} indicator (K_d = 600 nM), photorelease of IP_3 in oocytes first triggered local Ca^{2+} release activity from independent IP_3R clusters (Ca^{2+} puffs). Ca^{2+} puff number increased sharply with photolysis strength (Figure 1A), progressively triggering abortive Ca^{2+} waves, which failed to spread across the imaging plane, and then global Ca^{2+} waves [7]. In eggs, identical experiments revealed three key differences (Figures 1A and 1B). First, the relative threshold needed to evoke Ca^{2+} release was higher (~4-fold, 18 ± 4 ms in oocytes versus 74 ± 11 ms in eggs). This lower sensitivity was not due to cytoplasmic rearrangements that attenuated photolysis stimuli; the dose-response relationship for release of caged fluorescein was similar in oocytes and eggs (Figure 1C). Second, Ca^{2+} puffs were rarely resolved—the local Ca^{2+} signaling architecture evident only 8 hr previously in oocytes had remodeled. Third, IP_3 elevations sufficient to evoke Ca^{2+} mobilization frequently generated a Ca^{2+} wave that propagated extensively throughout the vegetal pole (i.e., the system was highly regenerative). Macroscopically, comparison of the magnitude and kinetics of Ca^{2+} waves via a low-affinity Ca^{2+} indicator (K_d = 3 μM) revealed that the peak amplitude of Ca^{2+} waves was greater and the duration of Ca^{2+} elevations more persistent in eggs than in oocytes (Figure 1D).

ER Densities Nucleate Ca^{2+} Signals in Eggs but Not Oocytes

In the same cells, vegetal ER morphology showed considerable reorganization during maturation. In oocytes, the monotypic cisternal organization of cortical ER har-

*Correspondence: march029@tc.umn.edu

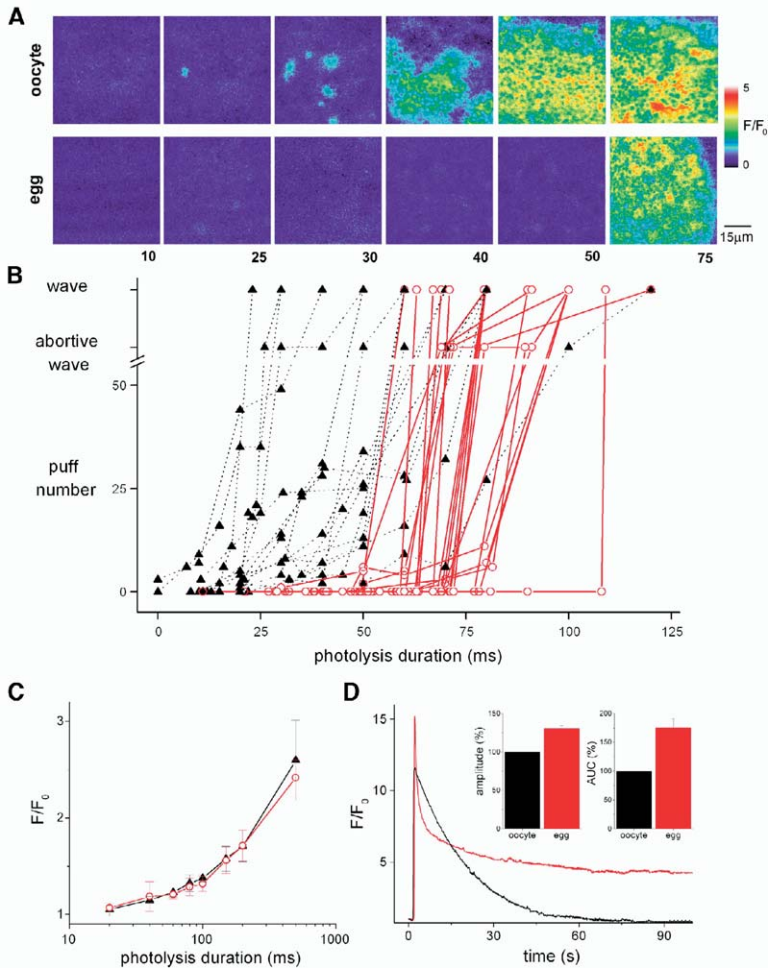

Figure 1. Remodeling of Ca^{2+} Signaling Dynamics during Maturation

(A) IP_3-evoked Ca^{2+} signals in the vegetal pole of an oocyte (top) and egg (bottom). Single frames show the spatial profile of Ca^{2+} release in response to photolysis flashes of the indicated durations (ms), measured with a high-affinity fluo4-dextran and depicted on a pseudocolor scale.

(B) From similar experiments, measurements depicting the number of active Ca^{2+} release sites (5-s period) after photolysis flashes of the indicated durations in oocytes (▲) and eggs (○). Responses are scored as the number of sites responding or as an abortive (the signal failed to propagate across the field) or global Ca^{2+} wave.

(C) Fluorescence-ratio increases evoked by photorelease of fluorescein.

(D) Maximal responses to IP_3 (flash strength = 10× wave threshold) in oocytes and eggs via a low-affinity fluo4-dextran. Responses were followed for ~90 s because cortical rotation precluded longer measurement.

Error bars reflect the standard error of the mean from n > 3 independent measurements.

boring Ca^{2+} puff sites had reorganized into "patch"-like densities (100–120 μm^3, 15 per 2500 μm^2, Figure 2A). Video-rate imaging correlating ER morphology with the sites of Ca^{2+} wave initiation showed that in all eggs tested (40 cells, 3 donors), the initial focus of IP_3-evoked Ca^{2+} release derived from an ER-rich density (Figure 2B; Movie S1 in the Supplemental Data available with this article online). Immunofluorescence staining for IP_3Rs revealed a high IP_3R load consistent within these ER densities, with their capacity to nucleate Ca^{2+} waves (Figure 2A).

In oocytes, the areas of highest ER density and IP_3R load were located in the subcortex (structures 10–20 μm long by 4 μm wide, 1 per 2500 μm^2, with a focal plane ~6 μm deep; Figure 2C). Dual-imaging experiments revealed the opposite phenotype to that seen in eggs—active Ca^{2+} release sites occurred throughout the ER, except in these domains of high ER density (Movie S2; summarized in Figure 2D). Live-cell staining with a GFP-tagged nucleoporin (Nup153-GFP) or tetramethylrhodamine-tagged wheat-germ agglutin (TMR-WGA) identified these ER-rich domains as annulate lamellae (AL) (Figure 2E). Although several functions have been proposed for AL, their prevalence in rapidly dividing cells has led to a consensus that AL act as nucleoporin repositories [8]. Surprisingly, dual-immunofluorescence labeling demonstrated a high content of full-length IP_3Rs within AL (Figure 2E) despite the lack of IP_3-evoked local Ca^{2+} release activity (Figure 2D). In summary, simultaneous imaging of ER structure and Ca^{2+} signals revealed two types of ER-rich and IP_3R-replete density in oocytes (i.e., AL) and eggs (i.e., patches), but with the incongruity that these structures displayed opposing Ca^{2+} release phenotypes (Figure 2D).

IP_3R-Replete Patches of ER in Eggs Derive from AL

The behavior of AL during maturation was followed by epifluorescence time lapse imaging in cells expressing Nup153-GFP or DsRed2-ER. In cells expressing Nup153-GFP, which selectively labels AL in the absence of wider ER staining, AL disappeared within 5 hr of progesterone addition (60%–70% of time to maturation [TTM]) and appeared to sink deeper into the cell (Figure 3A, Movie S3). A similar behavior was observed in cells expressing DsRed2-ER, with the sinking of AL preceding the appearance of the ER patches in the mature egg (~80% TTM; Figure 3A and Movie S4). Although the optical turbidity of oocytes prevented resolution of AL after its sinking in the majority of cells, there existed enough variability in the depth to which AL sank that it

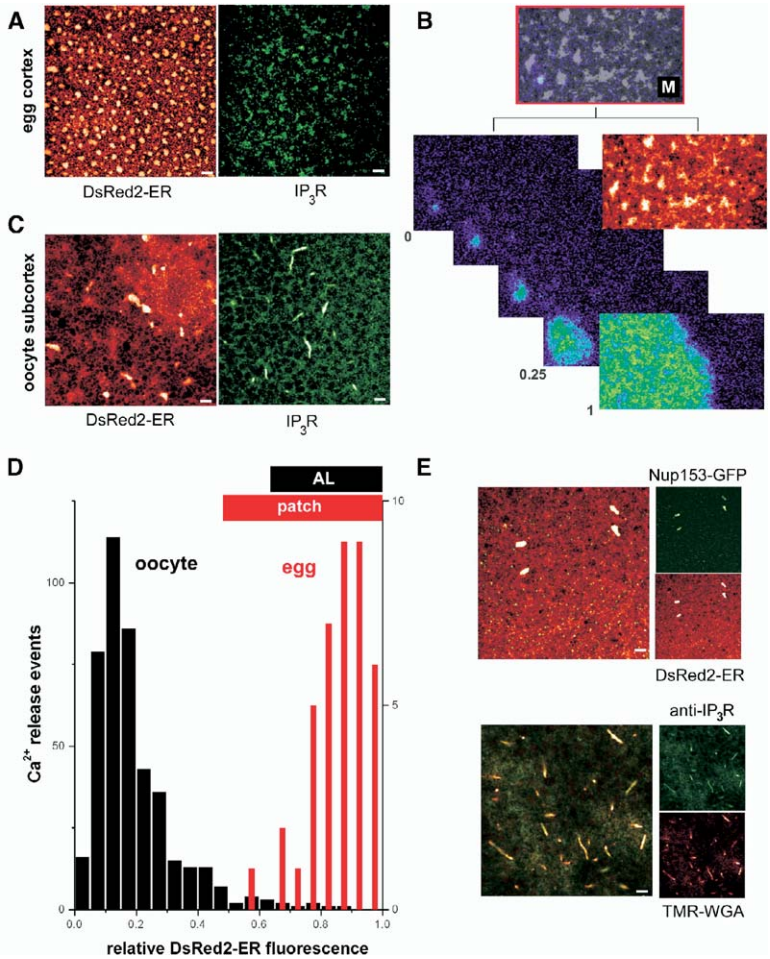

Figure 2. Correlation of ER Ultrastructure with Ca^{2+} Signaling Architecture

(A) Confocal images (*xy*) of ER (red) and IP_3R (green) distribution in egg cortex. The scale bars represent = 10 μm.

(B) Ca^{2+} wave initiation from ER- and IP_3R-rich patches in eggs (see overlay; M: see Movie S1) resolved by simultaneous monitoring of ER (red) and IP_3-evoked Ca^{2+} signals (time in seconds, pseudocolor).

(C) ER and IP_3R distribution in the oocyte subcortex.

(D) Relationship between DsRed2-ER fluorescence and Ca^{2+} release activity made by correlating the site of Ca^{2+} wave initiation (eggs, red) or Ca^{2+} puffs (oocyte, black) with underlying ER intensity normalized to the peak value in the same image plane. The ranges of DsRed2-ER values corresponding to patches and AL are shown.

(E) ER- and IP_3R-rich densities in oocytes are AL. The top shows an overlay in dual-expressing live cells of Nup153-GFP and DsRed2-ER. The bottom shows immunofluorescence of IP_3Rs and AL (stained by TMR-WGA, 4 μg/ml).

was possible to resolve the fate of AL in a small proportion of cells. In such cells, AL dispersed within ~6 hr of progesterone exposure (i.e., during the sinking period that preceded patch appearance), with the AL-derived fragments forming ER patches in the matured egg (Figure 3C, Movies S5 and S6). Direct visualization of IP_3R-rich AL fragments nucleating IP_3R-rich patches in the mature egg showed how AL organization was rapidly remodeled by physiological cues on a timeframe that paralleled ER redistribution into the maturing egg cortex [6].

Furthermore, treatment of DsRed2-ER-expressing oocytes with the weak base procaine (10 mM) resulted in cells lacking AL [4]. Because procaine likely mimics normal maturation events by causing a cytoplasmic alkalination similar to that of progesterone ([0.18 pH] increase; [9]), it is unsurprising that this stimulus applied with inappropriate timing or context interferes with ER remodeling. When matured with progesterone, these cells produced eggs without cortical-ER patches (Figure 3B), underscoring an interdependence between the two types of ER density.

AL Are a Functional Ca^{2+} Store, but One Where IP_3R Activity Is Attenuated

Given that the IP_3R-replete patches that initiate Ca^{2+} waves in eggs derive from AL, how is it that IP_3R activity is attenuated in AL whereas proximal ER supports Ca^{2+} puff activity? Our initial hypothesis was that AL were a physically distinct ER compartment in which IP_3R activity was attenuated by the high nucleoporin density, the ionic permeability of which depleted lumenal Ca^{2+}. During maturation, segregation from nucleoporins or reintegration into cortical ER competent at Ca^{2+} homeostasis resulted in increased IP_3R activity. However, two pieces of evidence suggested that the mechanisms that regulate IP_3R activity were more elegant than this simple model.

First, we tested whether AL were in lumenal continuity with the surrounding ER. Ever since the first ultrastructural studies were undertaken more than 50 years ago, electron micrographs have suggested an intimate relationship between AL and ER [8] to the extent that structural continuity between both structures has been implicity assumed but not previously demonstrated in live cells. Confocal images of DsRed2-ER morphology were suggestive of a structural interrelationship—in low-power scans, streams of ER could be tracked as if they were emanating from AL (Figure 3D). Higher-magnification images revealed ER structures shrouding the boundaries of individual AL (Figure 3D). To probe this relationship directly, we monitored DsRed2-ER fluorescence recovery in AL after photobleaching. Fluorescence recovered rapidly into AL (half-time ~45 s) when

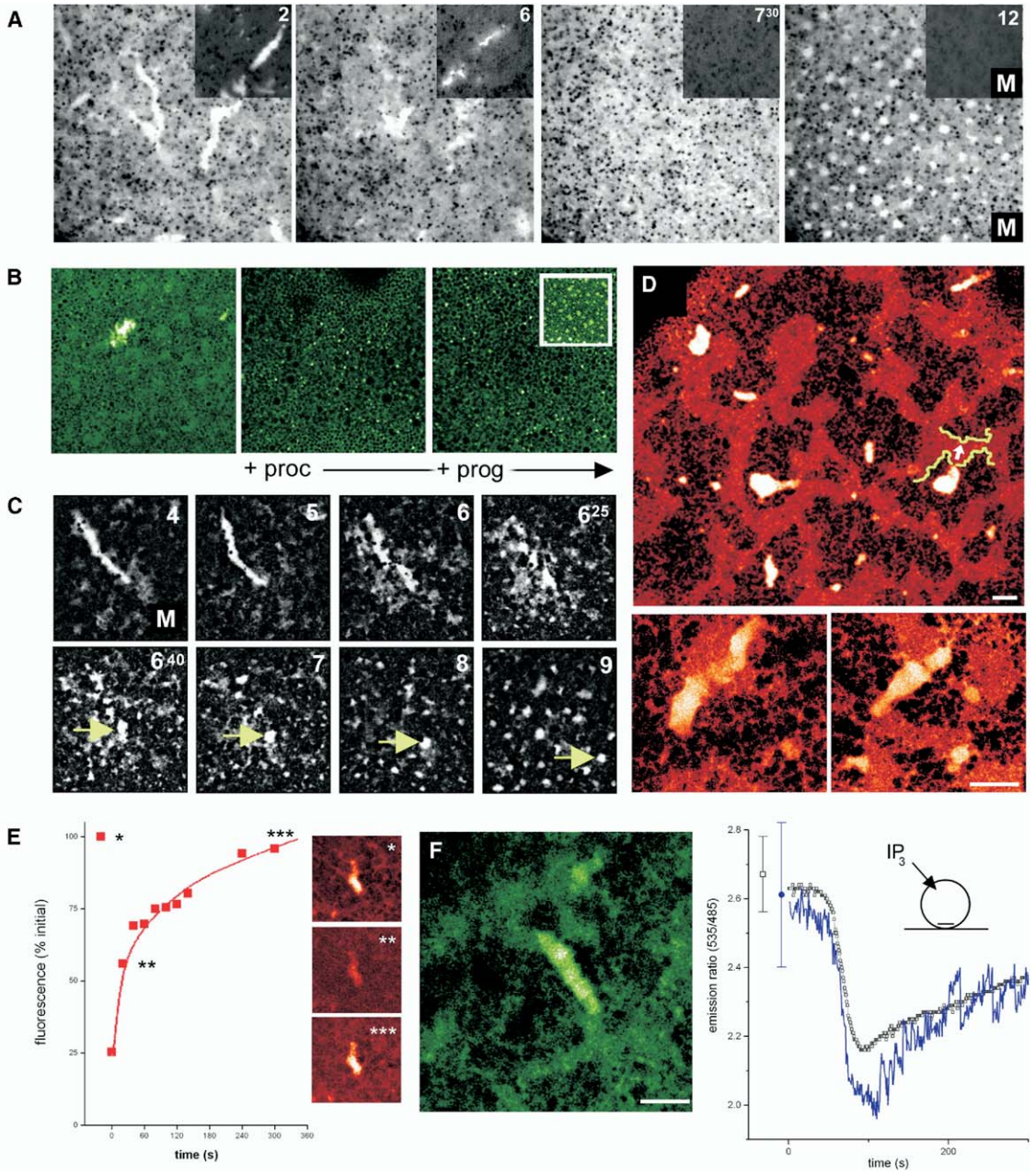

Figure 3. Cell Biology of AL

(A) Timelapse images of DsRed2-ER-expressing or Nup153-GFP-expressing (inset) cells at the indicated times (hr) after progesterone addition (M: see Movies S3 and S4).

(B) Oocyte expressing DsRed2-ER incubated with procaine (10 mM, middle) and then progesterone (right) failed to form ER patches. In the inset, patches form in control cells matured without procaine.

(C) ER patches derive from AL (M: see Movies S5 and S6). Timelapse (time in hours) images of AL monitored with DsRed2-ER to show the interrelationship between AL and patches (arrows) are shown.

(D) Confocal (*xy*) image of a DsRed2-ER-expressing oocyte to show AL at low and high magnification (the scale bars represent 10 μm). Annotation highlights ER emanating from an AL.

(E) DsRed2-ER fluorescence intensity from within an AL after photobleaching of a surrounding volume. Images at indicated times (asterisks) from a representative experiment are shown.

(F) Ca^{2+} dynamics in AL. At top, YC3.3-ER expression in the vegetal pole is shown. At right, ratiometric measurement of YC3.3-ER responses from a single AL (blue) or surrounding ER (black) to IP_3 injection in the animal pole (pipette, 1 mM) are shown. Single data points show average initial emission ratio and standard error.

AL and a surrounding volume of ER were photobleached, confirming a luminal continuity and underscoring the idea that AL should be considered as heterogeneous ER subdomains rather than as discrete organelles (Figure 3E). Second, we investigated Ca^{2+} dynamics within AL via ratiometric imaging of cameleon constructs. These probes are genetically-encoded FRET-based reporters, several members of which have Ca^{2+} affinities low enough to monitor Ca^{2+} concentrations within the ER (e.g., YC3.3-ER and YC4.0-ER) [10]. Nuclear injection of either construct resulted in fluorescence expression throughout the ER and within AL (Figure 3F). The resting fluorescence ratio of YC3.3-ER was higher than that of YC4.0-ER in wide-field measurements (2.6 ± 0.2 versus 2.1 ± 0.2, n = 4), paralleling the differential affinities of these probes for Ca^{2+} in vitro (YC3.3, low μM; YC4.0, tens of μM). At rest, the YC3.3-ER emission ratio (535/485 nm) was similar in AL and surrounding ER (Figure 3F), and microinjection of saturating IP_3 concentrations evoked a rapid decrease of this ratio in both AL (12.1% ± 3.7%) and neighboring ER (13.8% ± 3.4%). Therefore, AL contain Ca^{2+} (Figure 3) and full-length IP_3Rs (Figure 2) but nevertheless show an attenuated Ca^{2+} signaling phenotype prior to their dispersal during maturation.

AL and Ca^{2+} Signaling

How do changes in AL dynamics relate to developmental physiology? In *Xenopus* oocytes, responses to IP_3 are smaller in the vegetal than the animal pole [11]; this is the result of an asymmetric IP_3R distribution that presages the functional polarity in phosphoinositide signaling integral to dorsoventral specification [12, 13]. However, this preestablished bias must not prevent propagation of the fertilization Ca^{2+} wave, triggered by sperm fusion in the animal pole, across the entire egg. Therefore, a shuttling of IP_3Rs into cortical-ER clusters prior to fertilization and a dispersion of these clusters after fertilization [5] may ensure successful propagation of the fertilization Ca^{2+} wave across the vegetal pole without manipulating the hemispheric bias in IP_3R number. The increased IP_3R load but decreased sensitivity imply a further level of spatial sophistication in the remodeling process, possibly attributable to the high local density of IP_3Rs in ER patches [14]. In contrast, ER in the animal pole undergoes little reorganization during maturation; the greater density and size of IP_3R clusters as well as the increased sensitivity postmaturation present an alternative architectural solution to support Ca^{2+} wave propagation [11, 15] while preserving the sensitivity gradient that ensures animal (higher)-to-vegetal (lower) vectorality. Future studies of the impact of AL dynamics on developmental Ca^{2+} signaling are warranted—AL are found in oocytes of many species, including humans, where abnormal AL assembly correlates with early developmental failure [16, 17]. More widely, AL are found in many somatic cells and especially in scenarios of rapid proliferative capacity (e.g., cancerous tissues and viral infection) [8, 18].

A second area of interest centers upon the structural and/or functional mechanisms by which IP_3R activity is attenuated within AL. Many regulatory inputs modulate IP_3R sensitivity [19]—for example, progesterone-induced inhibition of adenylate cyclase is an early event in *Xenopus* maturation, and PKA phosphorylation modulates both IP_3R sensitivity and cellular localization [20]. Endogenous protein regulators that associate within the IP_3 binding domain could also modulate local IP_3R sensitivity [19]. Most intriguing is the observation that pre-MPF (Cdc2/CyclinB2) associates with AL in *Xenopus* oocytes whereas active MPF, which plays a mechanistically undefined role in ER remodeling, is soluble [21–23]. Recently, Cdc2 has been shown to phosphorylate mouse-brain IP_3R-1 at consensus sites (Ser^{421}, Thr^{799}) preserved in *Xenopus* IP_3Rs [24]. Dissecting the relevant mechanism(s) as well as understanding how these regulatory cues are selectively targeted to AL are the next steps in understanding how the functional architecture of Ca^{2+} signaling can be rapidly remodeled.

Conclusions

We have demonstrated a novel role for AL as an IP_3R-replete Ca^{2+} store involved in remodeling cellular Ca^{2+} dynamics. This new perspective on AL behavior underpins an elegant paradigm in which the spatiotemporal reorganization of cellular Ca^{2+} signaling observed during maturation is driven by subcellular redistribution of IP_3Rs rather than by molecular or familial Ca^{2+} channel diversity or changes in Ca^{2+} channel load.

Supplemental Data

Supplemental Experimental Procedures and six movies are available with this article online at http://www.current-biology.com/cgi/content/full/15/8/765/DC1/.

Acknowledgments

The authors were supported by National Institutes of Health grant NS046783 and a National Science Foundation CAREER Award to J.S.M. (0237946). We would like to thank Roger Tsien (University of California at San Diego) and Jan Ellenberg (European Molecular Biology Laboratory) for their generous gifts of reagents.

Received: January 26, 2005
Revised: February 25, 2005
Accepted: February 28, 2005
Published: April 26, 2005

References

1. Kume, S., Muto, A., Aruga, J., Nakagawa, T., Michikawa, T., Furuichi, T., Nakade, S., Okano, H., and Mikoshiba, K. (1993). The *Xenopus* IP_3 receptor: Structure, function and localization in oocytes and eggs. Cell *73*, 555–570.
2. Parys, J.B., Sernett, S.W., DeLisle, S., Snyder, P.M., Welsh, M.J., and Campbell, K.P. (1992). Isolation, characterization and localization of the inositol 1,4,5-trisphosphate receptor protein in *Xenopus laevis* oocytes. J. Biol. Chem. *267*, 18776–18782.
3. Kume, S., Yamamoto, A., Inoue, T., Muto, A., Okano, H., and Mikoshiba, K. (1997). Developmental expression of the inositol 1,4,5-trisphosphate receptor and structural changes in the endoplasmic reticulum during oogenesis and meiotic maturation of Xenopus laevis. Dev. Biol. *182*, 228–239.
4. Bement, W.M., and Capco, D.G. (1990). Transformation of the amphibian oocyte into the egg: Structural and biochemical events. J. Electron Microsc. Tech. *16*, 202–234.
5. Terasaki, M., Runft, L.L., and Hand, A.R. (2001). Changes in organization of the endoplasmic reticulum during *Xenopus* oocyte maturation and activation. Mol. Biol. Cell *12*, 1103–1116.
6. Campanella, C., Andreuccetti, P., Taddei, C., and Talevi, R.

(1984). The modifications of cortical endoplasmic reticulum during in vitro maturation of *Xenopus laevis* oocytes and its involvement in cortical granule exocytosis. J. Exp. Zool. *229*, 283–293.

7. Marchant, J.S., Callamaras, N., and Parker, I. (1999). Initiation of IP_3 mediated Ca^{2+} waves in *Xenopus* oocytes. EMBO J. *18*, 5285–5299.
8. Kessel, R.G. (1992). Annulate lamellae: A last frontier in cellular organelles. Int. Rev. Cytol. *133*, 43–120.
9. Lee, S.C., and Steinhardt, R.A. (1981). pH changes associated with meiotic maturation in oocytes of *Xenopus laevis*. Dev. Biol. *85*, 358–369.
10. Griesbeck, O., Baird, G.S., Campbell, R.E., Zacharias, D.A., and Tsien, R.Y. (2001). Reducing the environmental sensitivity of yellow fluorescent protein. J. Biol. Chem. *276*, 29188–29194.
11. Callamaras, N., Sun, X.-P., Ivorra, I., and Parker, I. (1998). Hemispheric asymmetry of macroscopic and elementary Ca^{2+} signals mediated by $InsP_3$ in *Xenopus oocytes*. J. Physiol. *511*, 395–405.
12. Kume, S., Muto, A., Inoue, T., Suga, K., Okano, H., and Mikoshiba, K. (1997). Role of the inositol 1,4,5-trisphosphate receptor in ventral signaling in *Xenopus* embryos. Science *278*, 1940–1943.
13. Saneyoshi, T., Kume, S., Amasaki, Y., and Mikoshiba, K. (2002). The Wnt/calcium pathway activates NF/AT and promotes ventral cell fate in *Xenopus* embryos. Nature *417*, 295–299.
14. Chang, K.-J., Jacobs, S., and Cuatrecasas, P. (1975). Quantitative aspects of hormone-receptor interactions of high affinity. Biochim. Biophys. Acta *406*, 294–303.
15. Machaca, K. (2004). Increased sensitivity and clustering of elementary Ca^{2+} release events during oocyte maturation. Dev. Biol. *275*, 170–182.
16. Sutovsky, P., Simerly, C., Hewitson, L., and Schatten, G. (1998). Assembly of nuclear pore complexes and annulate lamellae promotes normal pronuclear development in fertilized mammalian oocytes. J. Cell Sci. *111*, 2841–2854.
17. Rawe, V.Y., Olmedo, S.B., Nodar, F.N., Ponzio, R., and Sutovsky, P. (2003). Abnormal assembly of annulate lamellae and nuclear pore complexes coincides with fertilization arrest at the pronuclear stage of human zygotic development. Hum. Reprod. *18*, 576–582.
18. Cordes, V.C., Reidenbach, S., and Franke, W.W. (1996). Cytoplasmic annulate lamellae in cultured cells: Composition distribution and mitotic behavior. Cell Tissue Res. *284*, 177–191.
19. Bosanac, I., Michikawa, T., Mikoshiba, K., and Ikura, M. (2004). Structural insights into the regulatory mechanism of IP_3 receptor. Biochim. Biophys. Acta *1742*, 89–102.
20. Pieper, A.A., Brat, D.J., O'Hearn, E., Krug, D.K., Kaplin, A.I., Takahashi, K., Greenberg, J.H., Ginty, D., Molliver, M.E., and Snyder, S.H. (2001). Differential neuronal localizations and dynamics of phosphorylated type 1 inositol 1,4,5-trisphosphate receptors. Neuroscience *102*, 433–444.
21. Beckhelling, C., Chang, P., Chevalier, S., Ford, C., and Houliston, E. (2003). Pre-M phase-promoting factor associates with annulate lamellae in *Xenopus* oocytes and egg extracts. Mol. Biol. Cell *14*, 1125–1137.
22. Stricker, S.A., and Smythe, T.L. (2003). Endoplasmic reticulum reorganizations and Ca^{2+} signaling in maturing and fertilized oocytes of marine protostome worms: The roles of MAPKs and MPF. Development *130*, 2867–2879.
23. FitzHarris, G., Marangos, P., and Carroll, J. (2003). Cell cycle-dependent regulation of structure of endoplasmic reticulum and inositol 1,4,5-trisphosphate-induced Ca^{2+} release in mouse oocytes and embryos. Mol. Biol. Cell *14*, 288–301.
24. Malathi, K., Kohyama, S., Ho, M., Soghoian, D., Li, X., Silane, M., Berenstein, A., and Jayaraman, T. (2003). Inositol 1,4,5-trisphosphate receptor (type 1) phosphorylation and modulation by Cdc2. J. Cell. Biochem. *90*, 1186–1196.